The dual influence of the reed resonance frequency and tonehole lattice cutoff frequency on sound production and radiation of a clarinet-like instrument

Erik Alan Petersen, Philippe Guillemain, Michaël Jousserand

The dual influence of the reed resonance frequency and tonehole lattice cutoff frequency on sound production and radiation of a clarinet-like instrument

Erik Alan Petersen,[1] Philippe Guillemain,[1] and Michaël Jousserand[2]
[1] *Aix-Marseille Université, CNRS, Centrale Marseille, LMA, Marseille, France*
[2] *Buffet Crampon, Mantes-la-Ville, France*

(Dated: 31 March 2022)

The internal and external spectra of woodwind reed instruments are partially determined by the tonehole lattice cutoff and reed resonance frequencies. Because they can impact the spectrum in similar ways, a study of one without accounting for the other risks incomplete or false conclusions. Here, the dual effects of the cutoff and reed resonance frequencies are investigated using digital synthesis with clarinet-like academic resonators. It is shown that the odd and even harmonics have similar amplitudes at and above the cutoff frequency or reed resonance frequency, which ever is lowest. However, because the resonators radiate efficiently at the cutoff, it has the additional role of reinforcing the amplitude of both the odd and even harmonics in the external spectrum. The spectra are analyzed using the single value descriptors playing frequency, spectral centroid, odd/even ratio, and brightness, as a function of the musician mouth pressure. Higher reed resonances correspond to higher values for all descriptors. The odd/even ratio and brightness increase with resonator cutoff frequency, whereas the spectral centroid exhibits more complicated trends. The reed resonance has a larger impact on the 'playing condition oscillation threshold', implying that it may have a more important role in sustaining auto-oscillation.

 [https://doi.org(DOI number)]

[XYZ] Pages: 1–12

I. INTRODUCTION

Like all instruments, the timbre of a woodwind results from a number of interacting parameters. Some of these, such as the blowing pressure within the mouth, are controlled by the musician, while others are innate physical characteristics of the instrument such as the geometry of the air column. Because it is difficult to independently vary only one aspect of an instrument/musician combination, it is often unclear how different parameters affect the resulting spectrum. This is especially true when two or more parameters affect the spectrum in a similar manner. For cylindrical single-reed instruments, two such parameters, the lowest reed resonance frequency f_r and the tonehole lattice (THL) cutoff frequency f_c, can lead to similar effects on the internal and external spectrum of an instrument; disentangling their dual effects is the subject of the current article. Indeed, the ambiguous results of a previous study[1] using real instruments demonstrates the difficulty of separating these two variables and motivates a systematic approach to the problem.

The THL of many woodwind instruments have a certain acoustic periodicity which leads to pass- and stop-bands within the air column[2–6]. At low frequencies, an acoustic wave traveling from the mouthpiece towards the toneholes will largely radiate and reflect from the closest open tonehole. The strong reflection from the first open tonehole allows for the interference that determines the low frequency modes which facilitate auto-oscillation. In contrast, higher frequencies are able to propagate past the first open tonehole at which point they radiate from subsequent toneholes and the bell, as well as reflect from various locations within the lattice. The cutoff frequency f_c that separates these two regimes is determined by the specific geometry (tonehole radii, chimney heights, inter-hole spacing, and main bore radius) of the THL and, for a clarinet, is approximately 1500 Hz[5].

Under normal playing conditions, the oscillation of the reed favors frequencies that correspond to the first several peaks of the input impedance. These low frequency peaks are shifted in frequency by changing the fingering of the THL, and therefore sounding pitch, of the note. The reed has its own natural frequencies, the lowest of which is considerably higher than the frequencies in the first register of the clarinet. For simplicity, only the lowest reed resonance frequency f_r is considered in the current model. It is difficult to experimentally measure f_r, although it may be estimated using various tools such as instrumented mouthpieces or artificial blowing machines[7–9]; classically reported values are between 2000-3000 Hz[1,10]. Values between 1000-2000 Hz are to be expected when the reed is supported by the lip[11], and previous values used in a numerical continuation approach include 1500 Hz[12]. However, one complication

that arises in determining the dynamical properties of the reed is that the reed/mouthpiece/lip system is inherently nonlinear, including the nonlinear characteristic linking the pressure in the mouthpiece to the flow through into the instrument, nonlinear contact forces between the reed and the lay of the mouthpiece, and the nonlinear material properties of the musicians lips. There is a trade-off between using a simple model for which the results can be easily interpreted, versus a more complex model that more accurately captures the nonlinear physical system, but which may result in unnecessary higher-order phenomena.

The THL f_c and f_r are both known to impact the spectrum of the clarinet[1]. However, their relative importance has not been systematically studied. Clarinets, which may be idealized as a quarter-wave resonator at low frequencies, generally have high-amplitude odd harmonics corresponding to the input impedance peaks and low-amplitude even harmonics due to the lack of support at the input impedance valleys. However, the THL f_c induces a "region of reinforced spectrum," for which the odd and even harmonics are of similar amplitude and are efficiently radiated into the surrounding environment[13]. This phenomena also occurs at the nominal cutoff of real instruments[1,14]. The f_r may also induce a reinforced amplitude for harmonics that are close in frequency[10]. Other aspects related to the f_r, such as the lip force and lip position, affect the pitch, sound level, and spectrum of the clarinet[11,15].

Determining the influence of f_c and f_r on the spectrum is challenging in the case of real instruments because neither one can be varied without potentially impacting other aspects of the instrument. This is especially true for f_c because any alteration requires a modification of the lattice geometry, likely damaging the instrument. In order to investigate the dual influence of the THL f_c and f_r, it is necessary to develop a methodology that allows the two parameters to be varied independently. While it is relatively straightforward to devise and construct resonators with a given cutoff frequency[6,16], the practical challenge of controlling the resonance frequency of a physical reed[17] remains a challenge. Therefore, the phenomenon is explored numerically in the current article. Choosing to use a numerical model allows for precise control of the variables of interest, although the results are largely valid for comparing the qualitative effects of each model parameter.

The methodology of the numerical experiment is presented in Section II. Because much of the protocol has been previously published (citations in relevant sections), only a truncated account sufficient to interpret the results is provided in the current article. Section III shows the effect of f_c and f_r on general characteristics of the internal and radiated spectrum. Analysis highlights how each parameter can influence different aspects of the spectrum. Single value descriptors of the spectrum (playing frequency, spectral centroid, odd/even ratio, and brightness), as well as an analysis relating to the oscillation threshold, are provided in Section IV. A discussion of the results and conclusions are covered in Section V.

II. METHODOLOGY

Digital synthesis is used to compare the competing effects of the cutoff frequency and reed resonance on both the internal and external pressure spectra of simplified clarinet-like resonators. This is preferred over other available methodologies such as an instrumented mouthpiece or an artificial blowing machine because it allows to unambiguously isolate the variables of interest, notably the reed resonance frequency. Similarly, the musician control parameters relating to the blowing pressure and embouchure can be fixed to precise values, which may be achieved with a blowing machine, but is generally not possible for real musicians to attain when using an instrumented mouthpiece. Furthermore, it obviates complications relating to spectra measurements in real environments, be it a laboratory space, anechoic chamber, or a musically appropriate hall[1,14,18].

While digital synthesis generally does not perfectly match experimental results, it is a robust method for evaluating the qualitative differences that arise when some aspect of an instrument is modified[19]. For this reason, it is an appropriate tool for the current study which seeks to isolate the effects of two specific variables. Similarly, it may be useful to instrument manufacturers who wish to evaluate a hypothetical modification of an existing or non-existing instrument, without accruing the cost and time associated with manufacturing prototypes.

A. Resonator design

The current experiment utilizes four cylindrical resonators that are designed to resemble a simplified version of the clarinet, originally developed by some of the current authors for a different study[13]. Three of the resonators include a geometrically regular THL comprising 10 toneholes, the geometry of which are chosen to induce a THL cutoff frequency at 1.0, 1.5, and 2.0 kHz, see Table I, hereafter referred to as $\mathcal{R}_{1.0}, \mathcal{R}_{1.5}$, and $\mathcal{R}_{2.0}$, respectively. The inter-hole spacing is kept constant so that equivalent fingerings produce approximately the same sounding frequencies for each resonator. The upstream length, or the section that is between the mouthpiece and the first hole of the lattice, is chosen to account for the THL length correction such that the note corresponding to all the toneholes being open has the same first input impedance peak frequency for each resonator. The fourth "resonator" (see below), referred to as $\mathcal{R}_{\text{cyl}}$ and used as a control, is a simple cylinder devoid of toneholes.

In order to generate enough data to make general comments regarding the spectrum, it is necessary to analyze the harmonic content of multiple notes. Therefore, the highest six notes of resonators $\mathcal{R}_{1.0}, \mathcal{R}_{1.5}$, and $\mathcal{R}_{2.0}$, out of the 11 available notes excluding forked fingerings, are considered in the analysis. This ensures that the lowest note considered still retains a lattice with five

Resonator	L (cm)	b (mm)	f_c (Hz)	Impedance peak frequency (Hz)	Inharmonicity (cents)
$\mathcal{R}_{1.0}$	39.9	2.5	1000	185.2; 172.8; 161.9; 152.3; 143.7; 136.1	2.2; 4.3; 6.4; 7.9; 10.4; 11.4
$\mathcal{R}_{1.5}$	41.7	4.0	1500	185.1; 172.6; 161.8; 152.2; 143.6; 136.0	9.3; 11.0; 10.7; 11.3; 12.8; 13.1
$\mathcal{R}_{2.0}$	42.6	5.8	2000	185.0; 172.6; 161.7; 152.1; 143.6; 136.0	11.2; 11.7; 12.4; 12.9; 13.2; 13.1
$\mathcal{R}_{\text{cyl}}$	L (cm): 45.2; 48.5; 51.8; 55.0; 58.3; 61.5			185.1; 172.6; 161.7; 152.1; 143.6; 136.0	11.8; 12.7; 13.5; 14.0; 14.0; 13.9

TABLE I. Summary of the geometry and acoustical characteristics of the four resonators used in the current article. All resonators have a common internal radius $a = 6.5$ mm. Resonators $\mathcal{R}_{1.0}, \mathcal{R}_{1.5}$, and $\mathcal{R}_{2.0}$ have a common inter-hole spacing $\ell = 32.6$ mm (center to center) and tonehole heights $h = 9.8$ mm, where the six notes are produced by closing the first five consecutive toneholes. In the bottom row are the six lengths used for $\mathcal{R}_{\text{cyl}}$ (no THL), chosen to have similar first input impedance peak frequencies as $\mathcal{R}_{1.0}, \mathcal{R}_{1.5}$, and $\mathcal{R}_{2.0}$, but no THL cutoff. The right columns provide the first input impedance peak frequency f_1 in Hz and the inharmonicity $1200\log_2(f_2/(3f_1))$ in cents for each of the six notes. It is worth noticing that, contrary to a real clarinet, the inharmonicity between the first two peaks is positive, but it does not change the results of the current study.

open holes, and therefore that the intended cutoff frequency is maintained throughout the scale. The purely cylindrical resonator $\mathcal{R}_{\text{cyl}}$ is simulated using six different lengths, each with a first input impedance peak frequency corresponding to those of the 6 fingerings of the other three resonators. The maximum difference for a given note's input impedance peak frequency across the four resonators is less than 3 cents.

Simulations were performed under two conditions: the 'realistic' case where the volume of the closed toneholes (the closed THL[20]) is included in the calculations and the 'academic' case where the volume is excluded, such that the section between the mouthpiece and the first open tonehole is perfectly cylindrical for all fingerings. The realistic case introduced complications because the inharmonicity between the first and second input impedance peaks was not the same for the different resonators. Specifically, the inharmonicity becomes larger for the higher cutoff frequency resonators used in this study due to the larger tonehole radii. It was found that this affected both the internal and external spectra, although the effect is subtle. When the tonehole volumes are included, at frequencies below cutoff, the amplitude of the odd harmonics tend to be lower while the amplitude of the even harmonics tend to be higher. This is expected because the harmonics of the playing frequency will not sample as close to the maxima (odd harmonics) and minima (even harmonics) of the input impedance when there is additional inharmonicity. Including the tonehole volumes has a lesser effect above the cutoff because the input impedance peaks are no longer harmonically related to the low frequency resonances, and are sampled more or less at random by the harmonics of the playing frequency. Additionally, excluding the closed tonehole volumes ensures that there is no closed THL filtering between the internal and external sound fields[20]. To minimize the complexity of the study, closed toneholes are not included in the simulation to better isolate the effect of the cutoff and reed resonance frequencies without the added complication of increased inharmonicity.

It is important to recall that the cutoff f_c is only defined for an infinite, lossless lattice, and therefore is always approximate for a finite, lossy resonator[2]. The implications of this assumption do not impact the current work because the resonators are designed using a physical model, which accurately simulates the standing waves that occur above the approximate cutoff for a real instrument (traversing the entire length of the resonator, rather than confined between the first open tonehole and the mouthpiece). Indeed, the results would be different if the resonator had a true cutoff (lossless, infinite lattice) above which no energy is reflected back towards the mouthpiece. The relaxed definition of a cutoff frequency in this work corresponds more closely to the case of a real instrument than the theoretical pass- and stop-bands in periodic media, especially considering that the tonehole lattice of a real clarinet is not strictly periodic[5]. Another difference between the academic resonators used here and a real clarinet is the absence of a bell, which will tend to efficiently radiate frequencies above the tonehole lattice cutoff, weakening the standing waves within the full bore of the instrument. Indeed, the standing waves above cutoff for the academic resonators can be seen in the transfer functions shown in Sect. III C; the weakened standing waves above cutoff for real clarinets, in part due to the bell, may be observed on the measured or simulated input impedance[21]. Further complicating this topic, clarinet bells have their own cutoff response at around 1500 Hz. Therefore, while it would be possible to include a bell in the resonator simulations, the academic solution is again prioritized to better isolate the two factors of interest in this study.

B. Simulation of the resonator characteristics

The passive acoustic response corresponding to the six notes on all four resonators is simulated using an extension of the Transfer Matrix Method (TMM) that is modified to include external interactions of apertures (toneholes and the termination) radiating into the same space, known as the Transfer Matrix Method with external Interactions (TMMI)[22].

This calculation was devised to simulate the input impedance

$$Z_0(\omega) = P_0(\omega)/U_0(\omega), \tag{1}$$

where $P_0(\omega)$ and $U_0(\omega)$ are the frequency domain ($\omega = 2\pi f$) acoustic pressure and flow at the input of the resonator. One advantage of the TMMI algorithm is that it also provides the pressure and flow in the nth radiating aperture $P_n(\omega)$ and $U_n(\omega)$[13]. For the resonators with a THL comprising 10 holes, $n = 11$ including the termination of the resonator; $n = 1$ for the simple cylinders.

These quantities can be used to calculate a number of useful relations, such as the transfer function between the input pressure or flow quantities to those in the radiating apertures:

$$H_{u,n}(\omega) = U_n(\omega)/P_0(\omega). \tag{2}$$

These transfer functions (any combination of $P_0(\omega)$, $U_0(\omega)$, $P_n(\omega)$, and $U_n(\omega)$) can be used to understand basic characteristics of the resonator beyond what is available from the input impedance alone. In particular, Eq. (2) can be used used to calculate the far field pressure at $P_{\mathrm{Ext},m}(\omega)$ due to a given mouthpiece pressure $P_0(\omega)$, treating each nth aperture as a monopole source and ignoring diffraction:

$$P_{\mathrm{Ext},m}(\omega) = \sum_{n=1}^{N} j\omega\rho \frac{H_{u,n}(\omega)P_0(\omega)}{4\pi r_{n,m}} e^{-jkr_{n,m}}. \tag{3}$$

Here, j is the imaginary unit, ρ is the density of the medium, $k = \omega/c$ is the wavenumber in free space with the speed of sound c, and $r_{n,m}$ is the distance between the nth radiating aperture and the mth observation position. This simplified radiation model corresponds well to measurements performed in an anechoic chamber[23].

C. Digital synthesis

A previously[24,25] developed digital synthesis model is used to simulate the discrete time domain behavior of each resonator coupled to a single reed mouthpiece, as it would be played by a musician. The synthesis results of an earlier version of the algorithm was validated against acoustic recordings produced by an artificial mouth as part of a timbre perception study[15].

The three primary variables describing the dynamical behavior of the instrument are the reed displacement $x(t)$, acoustic pressure $p_0(t)$, and acoustic flow $u_0(t)$ at the input of the resonator

$$x(t) = \frac{\hat{x}(t)}{H}, p_0(t) = \frac{\hat{p_0}(t)}{p_M}, u_0(t) = z_c \frac{\hat{u_0}(t)}{p_M}, \tag{4}$$

where H is the height of the reed channel at rest, p_M is the pressure required to close the reed channel completely, and z_c is the characteristic impedance of the resonator. The three primary variables are dimensionless, while the hat notation is used for the physical value of each variable. The subscript used for the acoustic pressure and flow indicate that they are the discrete time domain representation of the frequency domain variables defined in Eq. (1) corresponding to the plane at the input of the resonator.

The dimensionless musician control parameters correspond to the mouth pressure γ and embouchure ζ enacted by the musician[26],

$$\gamma = \frac{p_m}{p_M}, \zeta = wHz_c\sqrt{\frac{2}{\rho p_M}}, \tag{5}$$

where p_m is the musician mouth pressure in physical units and w is the width of the reed channel. The reed is treated as a single degree of freedom oscillator[27]:

$$\frac{1}{2\pi f_{\mathrm{r}}}\ddot{x} + \frac{q_{\mathrm{r}}}{2\pi f_{\mathrm{r}}}\dot{x} + x = p_0(t) - \gamma + F_{\mathrm{c}}(x), \tag{6}$$

where f_{r} and q_{r} are the resonance frequency and damping coefficient of the reed. It is possible to include higher reed modes: the next lowest, which is also flexural, is approximately 2.6 times the first resonance[7]. However, harmonics in this frequency range (2600-5200 Hz, depending on the first resonance) are generally more than 40 dB below the fundamental, and are therefore of secondary importance compared to the effect of the first reed resonance and THL cutoff frequency. A contact force F_{c} between the reed and the mouthpiece lay[28] is defined by

$$F_{\mathrm{c}} = K_{\mathrm{c}}\left(\frac{x + 1 - |x+1|}{2}\right)^2 (1 + \beta\dot{x}), \tag{7}$$

where $K_{\mathrm{c}} = 100$ and $\beta = 5\text{e-}4$ are nonlinear stiffness and damping coefficients, respectively. Note that the contact force is only activated when $x \leq -1$, corresponding to the condition for which the reed is in contact with the lay of the mouthpiece[28,29].

The flow through the reed channel is linked to the pressure differential between the bore and the mouth of the player:

$$u_0(t) = \zeta\left(\frac{x(t) + 1 + |x(t)+1|}{2}\right)\mathrm{sign}(\gamma - p_0(t))\sqrt{\gamma - p_0(t)}. \tag{8}$$

In order to regularize the nonsmooth functions of Eqs. (7) and (8), each absolute value term $|\Lambda|$ (for an arbitrary argument Λ) is replaced by $\sqrt{\Lambda^2 + \eta}$, where $\eta = 0.01$ is a small regularization quantity[30]. Note that this model is inherently nonlinear, and that the regularization term likely captures a more realistic reed/lay interaction than the simplest single degree of freedom reed model[17,27,31]. It has been checked that the specific value chosen for η does not alter the qualitative trends observed in the synthesized spectra. However, the values may impact the emergence of higher registers. While this is not a concern for the academic resonators used in the current study, it may become important with realistic instrument geometries, particularly with the addition of narrow register holes.

The resonator is modeled by a reflection function formalism that is computed from the inverse Fourier transform of the reflection coefficient, which is itself determined by the input impedance[32]. This is preferential to a truncated modal representation because it includes

high frequencies in the synthesis, which is of particular importance when considering the effect of the THL cutoff frequency.

D. Numerical experiment

The six notes for each resonator are synthesized with a duration of 10 seconds using different reed resonance values equal to 1000 Hz, 1500 Hz, and 2000 Hz (audio examples provided in online supplementary material). These values are chosen to be approximately those of a clarinet, but with a wide enough range to observe their effect on the resulting waveform. The dimensionless musician control parameters corresponding to mouth pressure and embouchure are set to central values of $\gamma = 0.7$ and $\zeta = 0.4$, and are both slowly varied by approximately 15 % in order to mimic the natural instability of a real musician. Only first register notes were observed, likely due to the resonators simple geometry, although other regimes may be produced for other combinations of musician control parameters.[29] The reed quality factor is fixed at $q_\mathrm{r} = 0.4$. These values, corresponding to a '*forte*' playing level, were chosen in order to ensure synthesized tones that have substantial energy in the high frequency harmonics.

The frequency domain mouthpiece pressure $P_0(\omega)$ is calculated from the time domain pressure $p_0(t)$ using the built in MATLAB *fft* function in 0.5 s intervals that are treated with a Hann window. Similarly, the internal flow spectrum $U_0(\omega)$ can be calculated from $u_0(t)$. Equation. (2) is used to determine the resulting flow in each aperture.

The external pressure $P_{\mathrm{Ext},m}(\omega)$ is calculated using Eq. (3) at $M = 100$ far field locations ($|r_{1,m}| = 10$ m $\forall m$), evenly distributed on a circle in the plane of the resonator with the first open tonehole at the origin. There is no need to account for observation positions outside the plane because each tonehole is assumed to radiate as a monopole and diffraction is ignored, resulting in an axis-symmetric directivity pattern. The total radiated pressure spectrum is approximated by the sum of the pressures at all 100 external observation locations:

$$\bar{P}_{\mathrm{ext}}(\omega) = \sum_{m=1}^{M} P_{\mathrm{Ext},m}(\omega). \tag{9}$$

This method is chosen in order to avoid problems associated with the strong directivity of the resonator at frequencies above the cutoff.

III. RESULTS I: GENERAL CHARACTERISTICS

A. Internal spectrum

Figure 1 shows the results for the resonators $\mathcal{R}_{1.0}, \mathcal{R}_{1.5}$, and $\mathcal{R}_{2.0}$ in the left three columns and $\mathcal{R}_{\mathrm{cyl}}$ in the right column, where the reed resonances are, from top to bottom, $f_\mathrm{r} = 1000, 1500$, and 2000 Hz. (The left to right order of the resonators is maintained in Figs. 2-6 and the top to bottom order of reed resonances is maintained in Fig. 2.) The square and circular data markers (online: black and red) denote the odd and even harmonics, respectively. The vertical axes are represented in normalized decibels: $20\log_{10}(|P_0(\omega)|)$, where the dimensionless pressure $P_0(\omega)$ is normalized by an implicit reference equal to unity.

The dual effects of the THL cutoff and reed resonance on the internal spectrum can be observed in Fig. 1: both appear to induce a boost in the amplitude of the even harmonics at, and above, either f_c or f_r, whichever is lower. The effect of the cutoff can be observed by comparing the gap between odd and even harmonics at the cutoff of each resonator: they tend to merge at 1000 Hz in the left panels, 1500 Hz in the middle-left panels, and 2000 Hz in the middle right panels, corresponding to the cutoffs of $\mathcal{R}_{1.0}, \mathcal{R}_{1.5}$, and $\mathcal{R}_{2.0}$. The effect of the reed resonance is more subtle and is most easily observed for $\mathcal{R}_{\mathrm{cyl}}$ in the right column, where there is a distinct bump in the even harmonics at each reed resonance. It can also be observed for resonators $\mathcal{R}_{1.5}, \mathcal{R}_{2.0}$. For example, the top panel for $\mathcal{R}_{1.5}$ shows a gap of approximately 20 dB at 1000 Hz while the bottom has a gap greater than 30 dB. A similar comment may be made for $\mathcal{R}_{2.0}$. It is less clear in the panels corresponding to $\mathcal{R}_{1.0}$, for which f_c is less than or equal to f_r for all combinations. Figure 1 demonstrates that, while both the THL cutoff frequency and the reed resonance cause a reinforcement of the even harmonics, the cutoff appears to be the stronger effect.

B. External spectrum

The external pressure spectrum for the four resonators and three reed resonances are shown in Fig. 2, where the columns and rows follow the same scheme as in Fig. 1. The vertical axis is proportional to Fig. 1. As with the internal spectrum, odd and even harmonics become more similar in amplitude at and above the reed resonance. The effect of the cutoff frequency, however, is more pronounced: in addition to boosting the amplitude of the even harmonics, it introduces a 'region of reinforced spectrum' at the cutoff frequency comprising both odd and even harmonics. Notice that the envelop of the spectrum around cutoff is highest for $\mathcal{R}_{1.0}$, and drops by 5-10 dB for $\mathcal{R}_{1.5}$ and $\mathcal{R}_{2.0}$. This is due to the natural decrease in harmonic envelop characteristic of a clarinet-like system[1].

Note that including higher reed resonances would likely have a subtle affect on the spectral envelop shown in Figs. 1 and 2. However, any influence would occur at frequencies (2600-5200 Hz) where the harmonics are already very weak. More importantly, the characteristics of the clarinet spectrum are particularly important between 1000 and 2000 Hz, where the amplitude of the odd and even harmonics become equal due to the cutoff and/or reed resonance. Higher reed resonances will not have the same degree of impact as the first reed resonance because the odd and even harmonics already have equal amplitudes at frequencies above the first resonance and

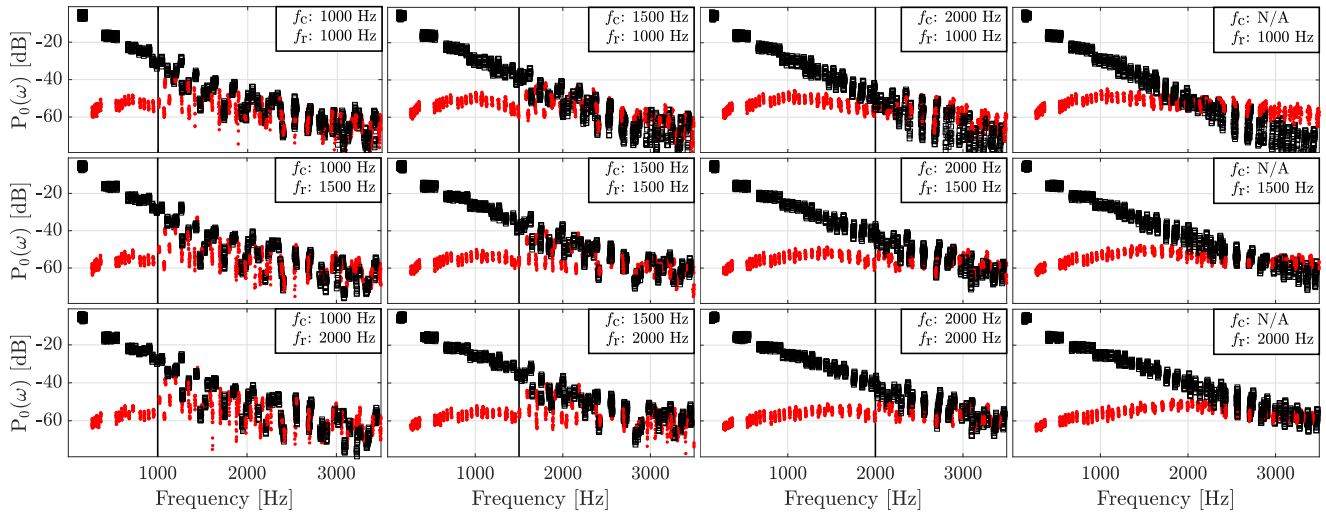

FIG. 1. (color online) Power spectra of synthesized non-dimensional pressure in the mouthpiece $P_0(\omega)$ for resonators with THLs $\mathcal{R}_{1.0}, \mathcal{R}_{1.5}$, and $\mathcal{R}_{2.0}$ (left three columns; f_c marked by vertical line) and no THL $\mathcal{R}_{\text{cyl}}$ (right column) for varying reed resonances $f_r = 1000, 1500, 2000$ Hz, from top to bottom. Each panel contains the spectra of six different notes with fundamental frequencies ranging from 136 Hz to 185 Hz, see Table I. Odd and even harmonics denoted by square (black) and circular (red) data markers, respectively.

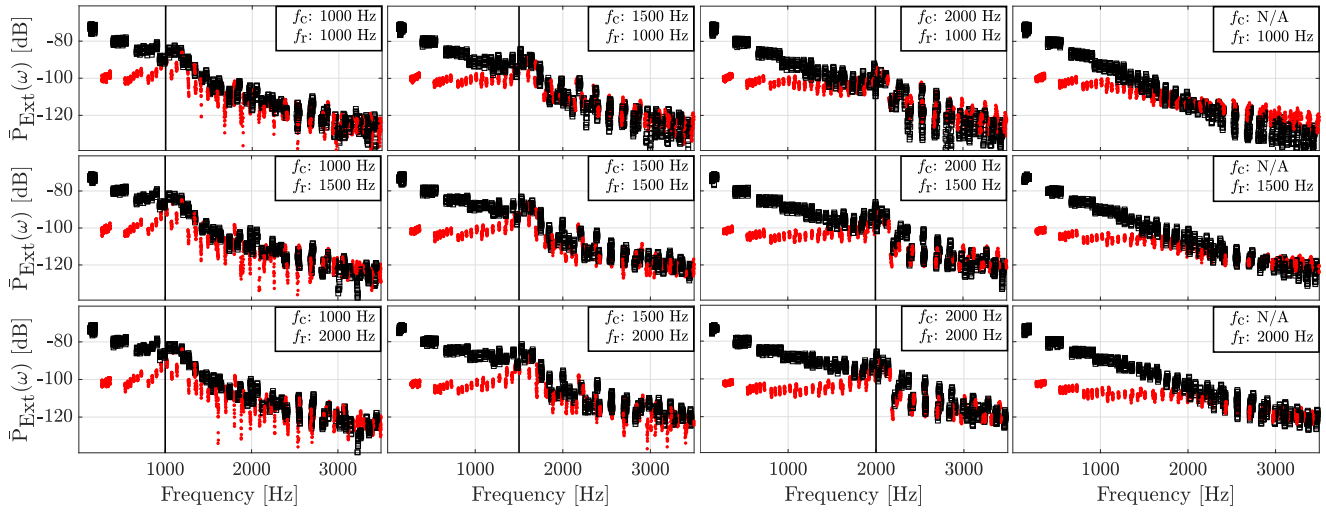

FIG. 2. (color online) Synthesized external non-dimensional pressure $\bar{P}_{\text{Ext}}(\omega)$ power spectra. Panel organization and pressure amplitudes relative to Fig. 1.

THL cutoff frequencies. That the spectrum has two principle frequency ranges (strong odd/weak even harmonics at low frequencies, parity at high frequencies) is likely an important perceptual characteristic of the clarinet.

C. The lattice as a filter

As seen in Sections III A and III B, the THL cutoff and reed resonance frequencies both impact the internal and external spectra by reinforcing the amplitude of the even harmonics. However, the external spectrum appears to be more strongly impacted by the THL cutoff frequency. Here, the effect of the THL as a filter is explored to better understand the distinction between the internal and external spectra.

Figure 3 shows the transfer function between the pressure in the mouthpiece and the summed time derivatives of the flow in each radiating aperture:

$$\mathrm{H}_{\text{rad}}(\omega) = \sum_{n=1}^{N} j\omega U_n(\omega)/P_0(\omega). \tag{10}$$

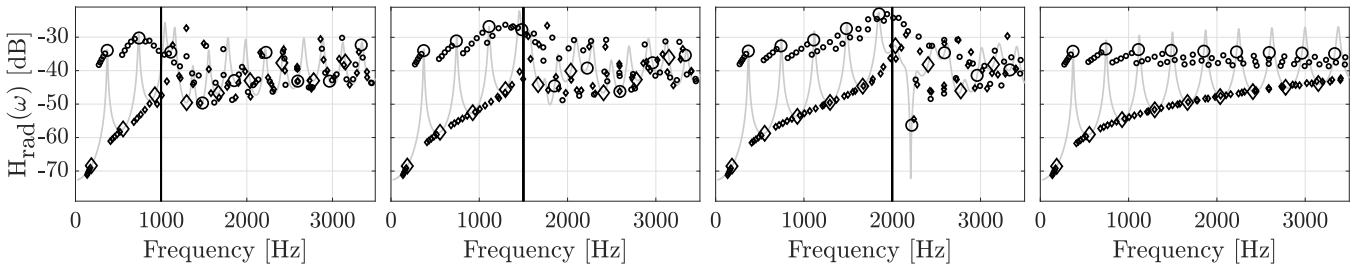

FIG. 3. Transfer function between the pressure at the input of the resonator and the sum of time derivative of the flow at each radiating aperture for, from left to right, resonators $\mathcal{R}_{1.0}, \mathcal{R}_{1.5}, \mathcal{R}_{2.0}$, and $\mathcal{R}_{\text{cyl}}$. This is an approximation of the transfer function between the mouthpiece pressure and the external sound field. The transfer functions are continuous in frequency and different for each fingering: for readability, only the highest fingering of each resonator is shown (grey line). The transfer function is sampled at integer multiples of the first input impedance peak, corresponding approximately to the harmonics in the spectrum, denoted by large diamonds (odd) and large circles (even) data markers. To reinforce the trends associated with cutoff (regardless of fingering), integer multiples of the first input impedance peak for the other five fingerings are depicted by small data markers.

To within a constant scaling factor, this expression is proportional to the transfer function between the internal pressure and farfield pressure ignoring diffraction, source separation, and spherical spreading, and is a reasonable approximation of general radiation characteristics that do not include the effects of directivity. Note that this is a passive characteristic of the resonator that depends solely on the geometry: the results are the same regardless of reed properties (such as resonance frequency) and other musician control parameters. The transfer function is calculated for all six notes of each resonator, but for clarity, only the highest note is shown in totality by the thin grey line. The first input impedance resonance frequency (corresponding approximately to the sounding frequency) is extracted for each fingering, and the transfer function $\mathrm{H}_{\text{rad}}(\omega)$ is sampled by integer multiples of this frequency with odd and even harmonics denoted by diamonds and circles, respectively. The large diamond/circle data markers correspond to the transfer function of the highest note, shown in grey.

The panels in Figure 3 demonstrate the impact of the THL on some radiation properties of the resonators. Below the cutoff, odd harmonics are radiated weakly compared to even harmonics, in accordance with the quarter-wave low frequency approximation of the resonator in which the lattice is ignored. At and above the cutoff, both the even and odd harmonics are efficiently radiated into the surrounding space. Resonator $\mathcal{R}_{\text{cyl}}$ demonstrates the extreme case, where the distinction between odd and even harmonics is maintained even at high frequencies.

Figure 4 shows the transfer function between the power flowing through the plane at the input of each resonator and the sum of the power flowing through each radiating aperture:

$$\mathrm{H}_{\Pi,n}(\omega) = \sum_{n=1}^{N} \mathrm{Re}\left[\frac{P_n(\omega)U_n^*(\omega)}{P_0(\omega)U_0^*(\omega)}\right], \tag{11}$$

where $*$ indicates the complex conjugate operation. All four resonators have approximately the same radiation efficiency below the cutoff and tend to converge to a similar value at high frequencies. There is a distinct increase in radiation efficiency at the cutoff of resonators $\mathcal{R}_{1.0}, \mathcal{R}_{1.5}$, and $\mathcal{R}_{2.0}$, which is not observed for $\mathcal{R}_{\text{cyl}}$.

These passive radiation characteristics, demonstrated by Figs. 3 and 4, provide the link between the internal and external spectra depicted in Figs. 1 and 2. While the reed resonance induces reinforced even harmonics in the nearby frequency band, it has no effect on the ability of the resonator to efficiently radiate these frequencies to the surrounding environment. The THL also induces reinforced even harmonics, but within a frequency band for which the resonator radiates efficiently. Therefore, both even and odd harmonics are reinforced in the radiated spectra. That the cutoff induces both of these effects is not to be viewed as a coincidence, but rather the dual results of an intertwined phenomena: because the resonator radiates efficiently at and above the cutoff frequency, the internally reflected waves that result in constructively interfering odd and destructively interfering even resonances no longer correspond to a quarter-wave resonator model. This allows even harmonics to be reinforced internally in addition to a strong radiation of both even and odd harmonics externally. Note that this is analogous to the interpretation that the harmonics of the playing frequency sampling the input impedance: below the THL cutoff, the odd harmonics tend to fall on or near peaks, while the even harmonics correspond primarily to valleys, while above cutoff, they are equally likely coincide with a peak or valley.

As seen in Fig. 3 (especially in the right panel which shows the lattice-less $\mathcal{R}_{\text{cyl}}$), the behavior deviates from this simple description at high frequencies. One cause is inharmonicity: the peaks and valleys of the input impedance do not coincide at perfect integer multiples of the first peak due to increased viscothermal losses at high

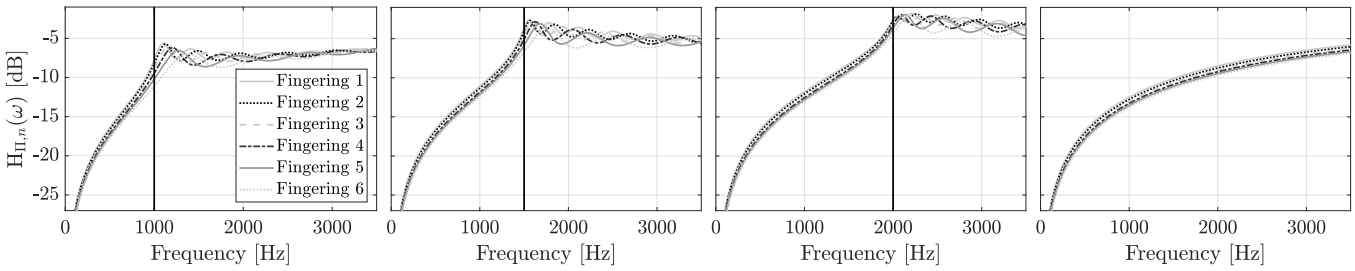

FIG. 4. Transfer function between the power flowing through the input of the resonator and the sum of the power flowing through the radiating apertures for, from left to right, resonators $\mathcal{R}_{1.0}, \mathcal{R}_{1.5}, \mathcal{R}_{2.0}$, and $\mathcal{R}_{\text{cyl}}$.

frequencies. This is also why the closed tonehole volumes are excluded in the simulations of the resonator; including those volumes increases the inharmonicity. Another reason is that higher frequencies radiate more efficiently than lower frequencies, so the transfer function increases up to the THL cutoff frequency of resonators $\mathcal{R}_{1.0}$, $\mathcal{R}_{1.5}$, and $\mathcal{R}_{2.0}$, and across the entire frequency band for $\mathcal{R}_{\text{cyl}}$. Above the THL cutoff, there is no simple application of this observation due to increased viscothermal losses as the sound wave reflects back and forth throughout the entire length of the resonator. Note that, under playing conditions, the playing frequency is always slightly lower than the first input impedance peak frequency so, even ignoring losses, the harmonics do not sample the input impedance exactly on the peaks and valleys.

IV. RESULTS II: SINGLE VALUE DESCRIPTORS OF THE SPECTRUM

The relative effect of the THL cutoff and the reed resonance frequencies on the internal and external spectrum is evaluated using objective descriptors. The purpose of this section is to demonstrate how the qualitative effects observed in Sect. III map to numerical descriptors that are often used for describing timbre. Here, the spectrum for each cutoff/resonance frequency combination is simulated for a wide range of normalized musician mouth pressures γ and fixed $\zeta = 0.4$, providing some insight on how the spectrum varies with the musician mouth pressure control parameter. Each signal is simulated for a duration of two seconds using a constant value for γ (in contrast to Section III), sufficiently long to extract the spectrum descriptors. Signals that are either unstable in pitch or sound outside of the first register are discarded.

The MIRtoolbox[33] is used to process the spectral characteristics of the internal and external soundfields. The external signal $\bar{P}_{\text{ext}}(\omega)$ is computed following the same procedure as in Section II B, from which the temporal signal is determined by the inverse Fourier transform assuming Hermitian symmetry in order to be processed as an audio file by the MIRtoolbox. A peak finding scheme (mirpeaks) is applied to identify the harmonic components of each signal. The spectral centroid, odd/even ratio, and brightness are computed from the harmonic power spectrum of the signal up to 9500 Hz, although choosing a lower value such as 5000 Hz does not change the qualitative trends because most of the energy in the signals is below 2000 Hz.

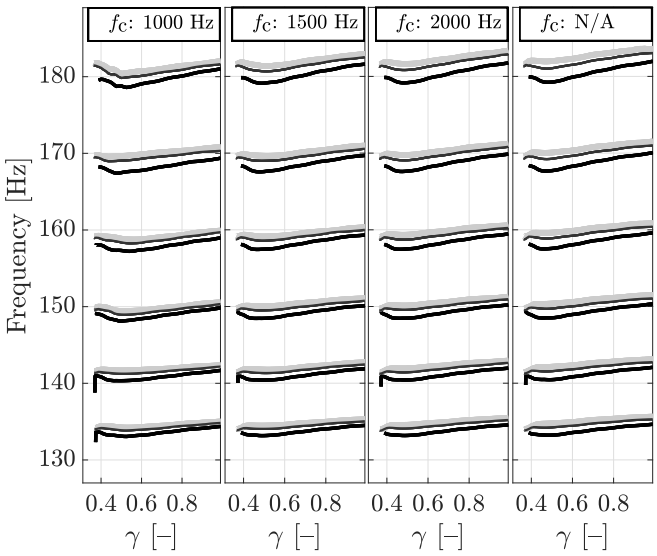

FIG. 5. Playing frequency as a function of musician mouth pressure γ for, from left to right, resonators $\mathcal{R}_{1.0}, \mathcal{R}_{1.5}, \mathcal{R}_{2.0}$, and $\mathcal{R}_{\text{cyl}}$. The thick black, thin black, and thick grey lines correspond to reed resonances $f_r = 1000, 1500$, and 2000 Hz, respectively.

A. Playing frequency

Figure 5 shows the playing frequency as a function of γ for the six notes considered on each of the four resonators. The thick black, thin black, and thick grey lines correspond to reed resonance frequencies $f_r = 1000$, 1500, and 2000 Hz, respectively. With a maximum discrepancy of approximately 17 cents for a given fingering, the six note 'scale' available to each resonator are reasonably similar in frequency, especially for the higher fingerings. This provides confidence that a comparison of spectrum characteristics across resonators is not likely to be com-

plicated by a difference in intonation, although it could induce difficulties in a subjective listening experiment.

Despite the significant differences in resonator geometries used in the current study compared with a real clarinet, the general trends seen in Fig. 5, such as the decrease in pitch up to $\gamma = 0.5$ followed by an increase in pitch for higher γ, is consistent with previous results[24,26]. The deviation in pitch from the first input impedance peak frequencies is likely primarily due to the inharmonicity between the first and second input impedance peaks and the reed induced flow, although the reed dynamics also play a role.[24] It is interesting to note that higher reed resonance frequencies result in higher playing frequencies for all four resonators.

B. Spectrum descriptors

Single value descriptors are extracted from the waveforms to determine global spectra differences due to the THL cutoff and reed resonance. The descriptors estimate the relative distribution of power between different sets of frequencies, calculated from harmonics extracted from the steady portion of the tone, discarding the transient. The first descriptor is the spectral centroid (SC),

$$\mathrm{SC} = \frac{\sum_{n=1}^{N} f_n A_n^2}{\sum_{n=1}^{N} A_n^2}, \tag{12}$$

which is often linked to the perceived 'brightness' of a tone[34]. The second descriptor, the odd/even ratio (OER), is the ratio between the power in the odd and even harmonics:

$$\mathrm{OER} = \frac{\sum_{n=1}^{N} A_{2n-1}^2}{\sum_{n=1}^{N} A_{2n}^2}. \tag{13}$$

A third descriptor, known as brightness (B_{3000}),

$$B_{3000} = \frac{\sum_{n(f\geq 3000)}^{N} A_n^2}{\sum_{n=1}^{N} A_n^2}, \tag{14}$$

is the fraction of the total power that is above some fixed cutoff frequency. Common values are 1000 Hz[35], 1500 Hz[33], and 3000 Hz[36]. For this article, the brightness calculation is in relation to a cutoff at 3000 Hz in order to be well above the THL cutoff and reed resonance frequencies. Therefore, this descriptor provides an indication of the variables effect on the high frequency portion of the spectrum, above the region of reinforced spectra (due to the THL) and above the frequency by which the odd and even harmonics have reached parity (due to either the THL or reed resonance).

Figure 6 shows the descriptors applied to the same THL cutoff and reed resonance configurations as in Figs. 1 and 2 as a function of the excitation pressure. The values shown correspond to the average of all six fingerings, thereby emphasizing the global spectra characteristics. The reed resonance categorically raises the values of all three descriptors regardless of resonator cutoff. It may be pointed out that higher reed resonances f_r also result in higher playing frequencies, which should naturally lead to higher descriptors of the spectra. However, it has been checked that the dimensionless SC (such that it has been normalized by the playing frequency) exhibits the same trends as the normal SC defined in Eq. (12). The OER and B_{3000} descriptors cannot be equivalently modified to account for different playing frequencies. However, because they quantify the high frequency content (B_{3000} is relative to 3000 Hz), it is unlikely that small variations in the playing frequency will influence the global qualitative trends.

1. Spectral centroid

As previously shown by some of the current authors, the SC of the internal spectrum increases with increasing THL cutoff frequency[16]. In contrast, there is not a monotonic increase in SC for increasing f_c for the external spectra. This may initially seem counter-intuitive: if it increases with internal spectra one might expect the same for the external spectra. Furthermore, Fig. 2 shows a region of reinforced spectra at the cutoff, so it is sensible to expect this to shift the SC higher for higher cutoffs. However, for a clarinet-like instrument, the vast majority of acoustical energy is contained in the low ranking harmonics. A low THL cutoff will create the region of reinforced spectra for harmonics that have a relative large fraction of the total energy compared to those in the region of reinforced spectra for the higher THL cutoffs. There is a complicated balance in the SC calculation between inherently high-energy low-ranking harmonics and boosting the inherently low-energy high-ranking harmonics. This indicates that the SC may not be a very useful descriptor to distinguish between the competing effects of the THL cutoff and the reed resonance frequency, especially in relation to human perception which is very sensitive to frequencies around 2000 Hz. However, it is worthwhile to note that $\mathcal{R}_{1.5}$, which has a cutoff that is most similar to real clarinets, has the largest range of SC available when considering different reed resonance frequencies. This suggests that an instrument with $f_\mathrm{c} \approx 1500$ Hz might have the most flexibility for finding an adequate timbre by using reeds with different mechanical properties.

2. Odd/even ratio

The OER is shown in the middle row of panels in Fig. 6. At low γ, this descriptor has very large values because the signal is primarily composed of the playing frequency, with very little energy in higher harmonics. As the pressure is increased, the value drops to a minimum value at approximately $\gamma = 0.5$ as other harmonics emerge. Above $\gamma = 0.5$, the value once again increases as the signal approaches the square-wave shape characteristic of a clarinet played at a high level[37,38].

Generally, the OER increases for resonators with higher THL cutoffs, and is the highest for the latticeless cylinder. Similarly, the OER also increases with

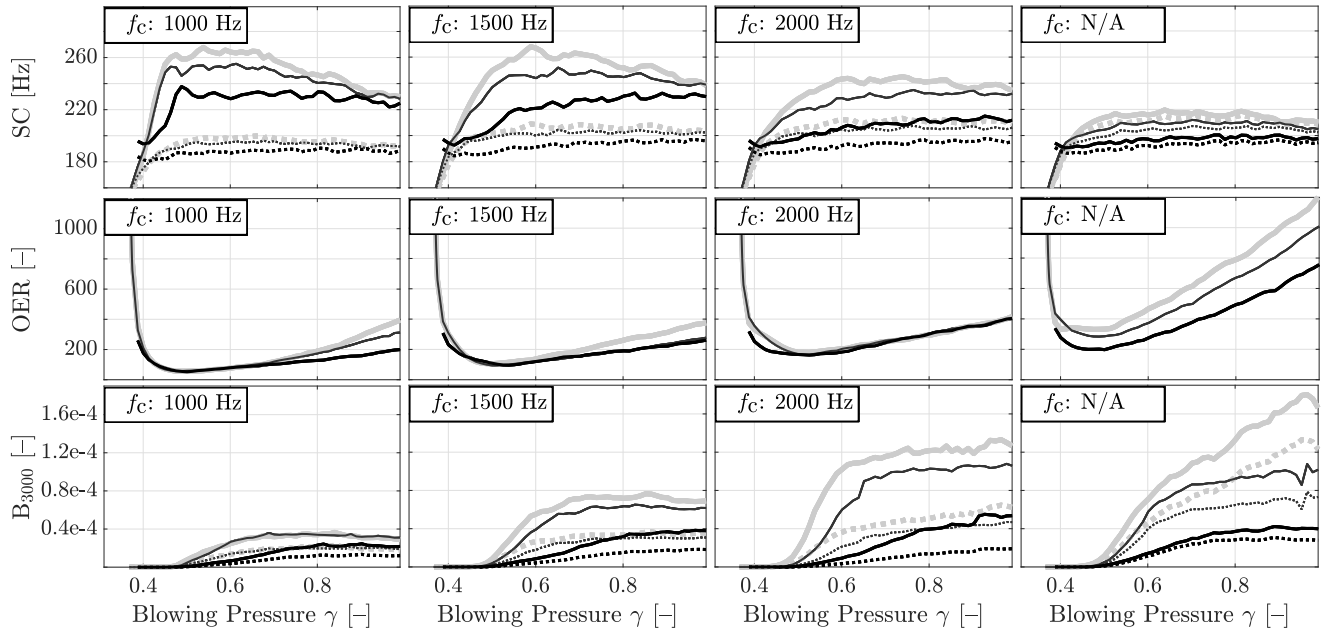

FIG. 6. Objective descriptors calculated from the harmonic power spectra of the synthesized waveforms as a function of blowing pressure γ for each THL cutoff and reed resonance frequency combination, averaged from the highest six fingerings of each resonator. Top: spectral centroid; Middle: odd/even ratio of harmonics; Bottom: Brightness relative to a cutoff at 3000 Hz. Left to right: $\mathcal{R}_{1.0}, \mathcal{R}_{1.5}, \mathcal{R}_{2.0}$, and $\mathcal{R}_{\text{cyl}}$. Reed resonance frequencies $f_r = 1000$, 1500, and 2000 Hz are denoted by thick black, thin black, and thick grey lines, which are solid for the external field and dotted for the internal field.

the reed resonance frequency. However, this narrative is challenged by the details: at high γ, the OER corresponding to $f_r = 1500$ Hz is higher for $\mathcal{R}_{1.0}$ than for $\mathcal{R}_{1.5}$. An interesting result is that the presence (or not) of a THL, regardless of it's cutoff frequency, appears to have the greatest impact on the OER. Resonators $\mathcal{R}_{1.0}$, $\mathcal{R}_{1.5}$, and $\mathcal{R}_{2.0}$ all have much lower OER than $\mathcal{R}_{\text{cyl}}$. For a lattice-less cylinder, the OER is strongly impacted by the reed resonance frequency, which is a much smaller effect for the other resonators. Although outside the scope of this study, it would be interesting to study how the presence of a bell, which is sometimes treated as a surrogate THL[21], would impact these results.

3. Brightness

The bottom panels of Fig. 6 show the brightness as defined by the MIR toolbox, not to be confused with the subjective use of this word to describe timbre. The brightness descriptor is perhaps the easiest to interpret: it increases with cutoff frequency and it increases with reed resonance. The conclusion is that both of these variables enable energy in the higher harmonics for both the internal and external spectra. The lattice-less resonator has brightness values that are greater than the resonators with a THL.

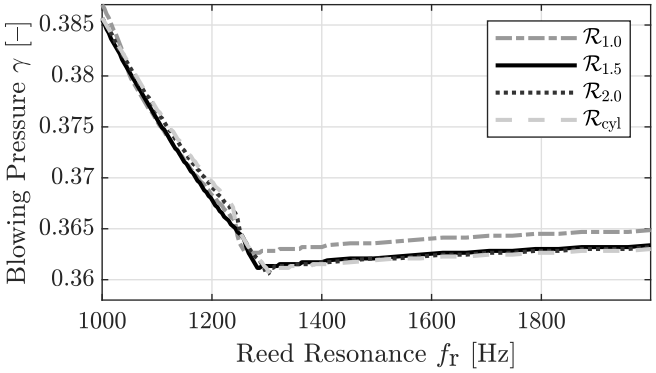

FIG. 7. Playing condition threshold of oscillation as a function of reed resonance frequency f_r for resonators $\mathcal{R}_{1.0}, \mathcal{R}_{1.5}, \mathcal{R}_{2.0}$, and $\mathcal{R}_{\text{cyl}}$.

C. Playing condition oscillation threshold

The threshold of oscillation, a parameter that is related to the 'playability' of an instrument, is known to be impacted by the reed resonance frequency[39,40], while the effect of the THL cutoff has, to the authors' knowledge, never been studied. Here, the phenomena is explored using a quantity that may be considered a 'Playing Condition Oscillation Threshold' (PCOT). Rather than studying the oscillation threshold using a slow pressure ramp or continuation scheme[12], the PCOT assumes that the

mouth pressure undergoes a rapid jump from $\gamma = 0$ to its final value. The PCOT is the lowest value of γ that results in a stable first regime oscillation for a given reed resonance frequency. Perhaps due to the relative simplicity of the resonators considered in this study, the second regime occurs very rarely, always close to the PCOT, and develops from an unstable first regime within several seconds. Therefore, the signals are synthesized for a duration of 10 seconds (as in Section II D) in order to disregard the γ values that result in this phenomenon. It is noted that a full bifurcation analysis is not the goal of the current study, which is mainly interested in the effect of f_c and f_r on the internal and external spectra.

In order to study the relative effects of the reed resonance and THL cutoff frequency, the PCOT is computed as a function of reed resonance frequency ($\zeta = 0.4$) for the four resonators. Figure 7 shows the results for the highest note of each resonator. The PCOT has a relatively high value when the reed resonance is less than 1200 Hz, drops rapidly to a minimum at approximately 1300 Hz and then rises slowly with increasing reed resonance frequency. It is interesting to note that, above 1300 Hz, $\mathcal{R}_{1.5}, \mathcal{R}_{2.0}$, and $\mathcal{R}_{\text{cyl}}$ have similar values while $\mathcal{R}_{1.0}$ has a uniformly higher value. The deviation for $\mathcal{R}_{1.0}$ may be due to the small number of low frequency input impedance peaks that facilitate in the auto-oscillation of the reed, making it harder to achieve oscillation. However, because the general trends are the same for all four resonators including the cylinder without a THL, it is reasonable to conclude that f_c is secondary to f_r in determining the PCOT.

The PCOT demonstrates a fundamental difference between the roles of the THL cutoff frequency and the reed resonance that is not evident when only considering the spectrum. While f_c appears to affect the spectrum more than f_r, it is the latter that may have the dominant role in sound production. This indicates that the 'ease of playing' and possibly articulation may be more closely linked to the reed resonance than the THL cutoff.

V. CONCLUSION

Digital synthesis using clarinet-like academic resonators shows that the tonehole lattice cutoff frequency f_c and reed resonance f_r impact the internal and external spectra. While they both lead to an increase in parity between the odd and even harmonics, the THL also induces increased radiation at its cutoff frequency. The single value descriptors of playing frequency, spectral centroid, odd/even ratio, and brightness all increase for higher reed resonance frequencies. The spectral centroid does not monotonically increase or decrease with the cutoff frequency. The ratio between the odd/even harmonics increases with both increasing tonehole lattice cutoff frequency and reed resonance. However, the presence of any tonehole lattice, regardless of it's cutoff, appears to be the greatest effect when compared with the lattice-less resonator. The brightness, corresponding to the ratio of power above 3000 Hz to the power below, does increase with cutoff frequency. These conflicting trends demonstrate that single value descriptors may not be a reliable tool to characterize the sounds of clarinet-like instruments. An analysis of the 'playing condition oscillation threshold' demonstrates that the reed resonance has a larger impact than the cutoff frequency on the minimum blowing pressure γ necessary for the emergence of first register oscillations. This indicates that the reed resonance may be the more important variable relating to the 'ease of playing' of a particular instrument.

A future study that would make these results practical for instrument manufacturers could involve listening experiments to link f_c and f_r to subjective impressions of the timbre. This poses two challenges: (1) controlling the mechanical properties of the reed is not easily achieved for real instruments; (2) digitally synthesized tones do not always produce realistic sounds, which could hinder their use in such a study. One possible solution may be to estimate the mechanical properties of a reed using an artificial mouth or instrumented mouthpiece[9,41], perhaps coupled to a cylindrical, lattice-less resonator, and observing trends in the amplitude of the even harmonics in the internal spectrum in comparison with synthesis results. An additional challenge for *in situ* experiments arises due to the variation in playing frequency caused by f_r; even a difference of 2 Hz (about 17 cents for the highest note of the resonators used in the current study) can complicate a subjective impression of 'brightness.' One could use a variable length L for the upstream portion of the resonator that can be adjusted to match the tuning of each note and reed resonance frequency, although the practicality of this solution is questionable. Finally, generalizations to real instruments should be made cautiously due to their more complicated THL geometries, which inherently have ambiguous cutoff frequencies. However, the THL cutoff is known to be an important characteristic of woodwind instruments, so the results in the current article likely remain applicable. Because the cutoff frequency has a strong impact on the external spectrum of an instrument, but only a minimal effect on the production of sound, it is conceivable that it may be utilized as a design parameter relating primarily to timbre.

Acknowledgement

The authors appreciate Tom Colinot and Jean Kergomard for their comments on the manuscript, and Jean-Pierre Dalmont for his insightful comments during an early stage of the project. This work has been partly supported by the French Agence Nationale de la Recherche (ANR16-LCV2-0007-01 Liamfi project).

[1] A. H. Benade and S. N. Kouzoupis, "The clarinet spectrum: theory and experiment," J. Acoust. Soc. Am. **83**(1), 292–304 (1988).

[2] L. Brillouin and M. Parodi, *Wave propagation in periodic structures* (Dover Publications, NY, USA, 1946).

[3] A. H. Benade, "On the mathematical theory of woodwind finger holes," J. Acoust. Soc. Am. **32**, 1591–1608 (1960).

[4]D. H. Keefe, "Woodwind air column models," J. Acoust. Soc. Am. **88**, 35–51 (1990).

[5]E. Moers and J. Kergomard, "On the cutoff frequency of clarinet-like instruments. Geometrical versus acoustical regularity," Acta Acust united Ac **97**, 984–996 (2011).

[6]E. Petersen, T. Colinot, J. Kergomard, and P. Guillemain, "On the tonehole lattice cutoff frequency of conical resonators: applications to the saxophone," Acta Acust. **4**(4), 13 (2020) doi: 10.1051/aacus/2020012.

[7]P.-A. Taillard, F. Laloë, M. Gross, J.-P. Dalmont, and J. Kergomard, "Statistical estimation of mechanical parameters of clarinet reeds using experimental and numerical approaches," Acta Acustica united with Acustica **100**(3), 555–573 (2014) doi: doi:10.3813/AAA.918735.

[8]A. Muñoz Arancón, "New techniques for the characterization of single reeds in playing conditions," Ph.D. thesis, Université du Maine, 2017.

[9]P.-A. Taillard, "Theoretical and experimental study of the role of the reed in clarinet playing," Ph.D. thesis, Le Mans Université, 2018.

[10]S. C. Thompson, "The effect of the reed resonance on woodwind tone production," The Journal of the Acoustical Society of America **66**(5), 1299–1307 (1979) doi: 10.1121/1.383448.

[11]A. Almeida, D. George, J. Smith, and J. Wolfe, "The clarinet: How blowing pressure, lip force, lip position and reed "hardness" affect pitch, sound level, and spectrum," The Journal of the Acoustical Society of America **134**(3), 2247–2255 (2013) doi: 10.1121/1.4816538.

[12]S. Karkar, C. Vergez, and B. Cochelin, "Oscillation threshold of a clarinet model: A numerical continuation approach," The Journal of the Acoustical Society of America **131**(1), 698–707 (2012) doi: 10.1121/1.3651231.

[13]Petersen, Erik Alan, Colinot, Tom, Guillemain, Philippe, and Kergomard, Jean, "The link between the tonehole lattice cutoff frequency and clarinet sound radiation: a quantitative study," Acta Acust. **4**(5), 18 (2020) doi: 10.1051/aacus/2020018.

[14]A. H. Benade and S. J. Lutgen, "The saxophone spectrum," J. Acoust. Soc. Am. **83**, 1900–1907 (1988).

[15]M. Barthet, P. Guillemain, R. Kronland-Martinet, and S. Ystad, "From clarinet control to timbre perception," Acta Acustica united with Acustica **96**, 678–689 (2010) doi: 10.3813/AAA.918322.

[16]E. Petersen, P. Guillemain, J. Kergomard, and T. Colinot, "The effect of the cutoff frequency on the sound production of a clarinet-like instrument," J. Acoust. Soc. Am. **145**(6), 3784–3794 (2019) doi: 10.1121/1.5111855.

[17]J.-P. Dalmont, J. Gilbert, and S. Ollivier, "Nonlinear characteristics of single-reed instruments: Quasistatic volume flow and reed opening measurements," The Journal of the Acoustical Society of America **114**(4), 2253–2262 (2003) https://doi.org/10.1121/1.1603235 doi: 10.1121/1.1603235.

[18]A. H. Benade, "From instrument to ear in a room: direct or via recording," J. Audio Eng. Soc. **33**(4), 218–233 (1985).

[19]N. Giordano and V. Chatziioannou, "Status and future of modeling of musical instruments: Introduction to the jasa special issue," The Journal of the Acoustical Society of America **150**(3), 2294–2301 (2021) doi: 10.1121/10.0006439.

[20]E. A. Petersen, T. Colinot, F. Silva, and V. H.-Turcotte, "The bassoon tonehole lattice: Links between the open and closed holes and the radiated sound spectrum," The Journal of the Acoustical Society of America **150**(1), 398–409 (2021) doi: 10.1121/10.0005627.

[21]"Website on musical acoustics maintained by Joe Wolfe" , http://www.phys.unsw.edu.au/jw/ accessed: 2021-10-15.

[22]A. Lefebvre, G. Scavone, and J. Kergomard, "External tonehole interactions in woodwind instruments," Acta Acustica united with Acustica **99** (2012) doi: 10.3813/AAA.918676.

[23]E. A. Petersen, "Wave propagation in periodic structures applied to woodwind tonehole lattices: How the cutoff frequency balances sound production and radiation," Ph.D. thesis, Aix Marseille Université, 2020.

[24]W. L. Coyle, P. Guillemain, J. Kergomard, and J.-P. Dalmont, "Predicting playing frequencies for clarinets: A comparison between numerical simulations and simplified analytical formulas," The Journal of the Acoustical Society of America **138**(5), 2770–2781 (2015) doi: 10.1121/1.4932169.

[25]T. Colinot, "Numerical simulation of woodwind dynamics: investigating nonlinear sound production behavior in saxophone-like instruments," Ph.D. thesis, Aix-Marseille Université, 2020.

[26]T. A. Wilson and G. S. Beavers, "Operating modes of the clarinet," The Journal of the Acoustical Society of America **56**(2), 653–658 (1974) doi: 10.1121/1.1903304.

[27]F. Avanzini and M. Van Walstijn, "Modelling the mechanical response of the reed-mouthpiece-lip system of a clarinet. part i. a one-dimensional distributed model," Acta Acustica united with Acustica **90**, 537–547 (2004).

[28]S. Bilbao, A. Torin, and V. Chatziioannou, "Numerical modeling of collisions in musical instruments," Acta Acustica united with Acustica **101**(1), 155–173 (2015) doi: doi:10.3813/AAA.918813.

[29]Colinot, Tom, Vergez, Christophe, Guillemain, Philippe, and Doc, Jean-Baptiste, "Multistability of saxophone oscillation regimes and its influence on sound production," Acta Acust. **5**, 33 (2021) doi: 10.1051/aacus/2021026.

[30]T. Colinot, L. Guillot, C. Vergez, P. Guillemain, J.-B. Doc, and B. Cochelin, "Influence of the "ghost reed" simplification on the bifurcation diagram of a saxophone model," Acta Acustica united with Acustica (2019).

[31]S. Ollivier, "Contribution à l'étude des oscillations des instruments à vent à anche simple [A contribution to the study of single reed woodwind instruments]," Ph.D. thesis, Université du Maine, 2002. Français, 2002, acoustique [physics.class-ph].

[32]B. Gazengel, J. Gilbert, and N. Amir, "Time domain simulation of single reed wind instrument. from the measured input impedance to the synthesis signal : Where are the traps?," Acta Acustica united with Acustica **3**, 445 (1995).

[33]O. Lartillot and P. Toiviainen, "A matlab toolbox for musical feature extraction from audio," in *Proc. of the International Conference on Digital Audio Effects, Bordeaux* (2007).

[34]E. Schubert and J. Wolfe, "Does timbral brightness scale with frequency and spectral centroid," Acta Acustica united with Acustica **92**, 820–825 (2006).

[35]P. Laukka, P. Juslin, and R. Bresin, "A dimensional approach to vocal expression of emotion," Cognition and Emotion **19(5)**, 633–653 (2005) doi: 10.1080/02699930441000445.

[36]P. N. Juslin, "Cue utilization in communication of emotion in music performance: relating performance to perception.," Journal of experimental psychology. Human perception and performance **26 6**, 1797–813 (2000).

[37]S. Ollivier, J. Kergomard, and J.-P. Dalmont, "Spectrum of cylindrica reed instruments: comparison between theory and experiment," in *Proc. of Int. Symp. Music Acous. (ISMA)* (2001).

[38]A. Chaigne and J. Kergomard, *Acoustics of Musical Instruments* (Springer-Verlag, New York, 2016) (English translation).

[39]F. Silva, J. Kergomard, C. Vergez, and J. Gilbert, "Interaction of reed and acoustic resonator in clarinetlike systems.," The Journal of the Acoustical Society of America **124 5**, 3284–95 (2008).

[40]F. Silva, "Émergence des auto-oscillations dans un instrument de musique à anche simple," Ph.D. thesis, Université de Provence - Aix-Marseille I, 2009, acoustique [physics.class-ph], Français.

[41]P. Guillemain, C. Vergez, D. Ferrand, and A. Farcy, "An instrumented saxophone mouthpiece and its use to understand how an experienced musician plays," Acta Acustica united with Acustica **96**, 622 – 634 (2010) doi: 10.3813/AAA.918317.